Fine structure of electron-transmission spectra across AlAs single barriers

E. L. Ivchenko and A. A. Kiselev
A. F. Ioffe Physico-Technical Institute, Russian Academy of Science, 194021 St. Petersburg, Russia

Y. Fu and M. Willander
Department of Physics and Measurement Technology, Linköping University, S-581 83 Linköping, Sweden
(Received 20 December 1993; revised manuscript received 19 May 1994)

We propose a general approach to the problem of intervalley mixing of electron states in heterostructures in the effective-mass method. The method has been used to calculate electron-transmission spectra across GaAs(AlAs)$_M$GaAs single-barrier structures taking into account the Γ-X mixing at interfaces. The spectra exhibit sharp peaks and dips connected with the electron resonant transmission through quasibound X-like states in the AlAs layer. The peak and dip sequence depends on the parity of M. The developed approach allows us to present the energy dependence of transmission probability in an analytical form. The low-temperature dc current-voltage characteristics of the single-barrier structure has been derived making allowance for the camel-back X-band structure in bulk AlAs and GaAs.

I. INTRODUCTION

At present, the GaAs/AlAs multilayer structure is a convenient model object to study intervalley mixings of electron states due to the lack of translational symmetry at heterointerfaces.[1] There have been numerous calculations of electron tunneling probabilities across GaAs/AlAs single- or double-barrier heterostructures taking into account the Γ-X mixing effects. These range from computations based on the tight-binding models[2–5] and those that use the empirical-pseudopotential tunneling formalism[6,7] to calculations within the generalized effective-mass approximation.[8–12] Theoretical transmission spectra show sharp peaks due to electron resonant tunneling via metastable X states. Such states exist because, for X-point electrons, the AlAs layer should be considered as a quantum well. An interesting feature of the spectra is that the resonant peaks can be preceded or followed by sharp dips (transmission zeros). However, only recently it has been realized[5,12,13] that the transmission spectra and, in particular, the relative position between a peak and its satellite dip depend on whether the AlAs layer contains an even or odd number of monomolecular layers. In Ref. 12 we used a generalized formulation of the effective-mass method proposed by Ando and Akera[9] (see also Ref. 8) and corrected by Aleiner and Ivchenko[14] to take into account different translational properties of Γ- and X-point Bloch functions. In the method, the mixing of Γ- and X-like states is described by extra terms in the boundary conditions of electron envelope functions, and the parity dependence arises because the phase of the Γ-X mixing coefficient changes by π if the interface is shifted along the principal axis by one monolayer. This sign alternation property was also pointed out by Ando recently.[15]

In this paper, we present a theoretical study of resonant tunneling through a GaAs(AlAs)$_M$GaAs structure where attentions are focused on the analytical properties of the electron transmission spectra (Sec. II), the transmission probability calculations in the perturbation theory (or sequential) approach (Sec. III) and the analytical description of the current vs voltage dependence taking into account a self-consistent electrostatic potential induced by the buildup of X electrons in the AlAs layer (Sec. IV).

II. TRANSMISSION THROUGH GaAs(AlAs)$_M$GaAs STRUCTURE

We start with a convenient form to represent electron reflectivity and transmissivity of a symmetric multilayer heterostructure. Let the structure contain a chain of layers in the region between $-z_0$ and z_0 (see Fig. 1) surrounded by semi-infinite, uniform and identical layers. In Fig. 1 we introduce the amplitudes of incoming and outcoming waves on the left and right sides. For the tunneling problem one can put $A^l_{\rm in} = 1$, $A^r_{\rm in} = 0$, in which case $A^r_{\rm out} = T$ and $A^l_{\rm out} = R$ are the amplitudes of trans-

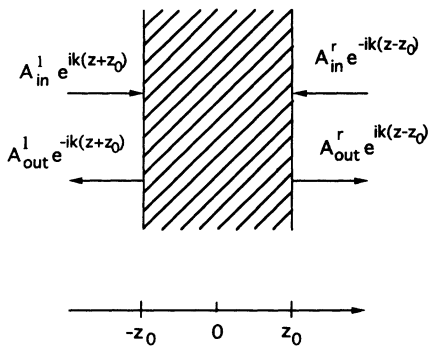

FIG. 1. Amplitudes of the incoming and outcoming electron waves.

mission and reflection waves.

The structure is assumed to be invariant under mirror reflection in the plane $z = 0$. This allows one to split the above problem into two auxiliary problems and to seek separately solutions of opposite parities with $A^l_{\rm in} = A^r_{\rm in} = 1$, $A^l_{\rm out} = A^r_{\rm out} \equiv r_+$ (even) and $A^l_{\rm in} = -A^r_{\rm in} = 1$, $A^l_{\rm out} = -A^r_{\rm out} \equiv r_-$ (odd). It is evident that T, R, and $r_\pm$ are interconnected by

$$T = (r_+ - r_-)/2,\ R = (r_+ + r_-)/2. \tag{2.1}$$

The main advantage of this representation is as follows: while calculating r_+ or r_-, one should take into consideration only a one-half of all linearly independent solutions inside the interval $(-z_0, z_0)$. In particular, this means that r_+ and r_-, as analytical functions of the initial electron energy, have poles at complex self-energies, respectively, for even and odd quasistationary states of quantum-confined electrons. Moreover, if there exist no other propagating waves outside the interval $(-z_0, z_0)$ one can show by using the electron flux conservation requirement that $|r_+| = |r_-| = 1$, and from whence $r_\pm$ can be treated as phase factors

$$r_+ = e^{i\phi_+},\ r_- = e^{i\phi_-}. \tag{2.2}$$

Note that Eqs. (2.1) and (2.2) are in agreement with the identity $\mathrm{Re}(R/T) = 0$ obtained for symmetrical systems (see Ref. 16).

Now we apply representation (2.1) to a double-interface structure GaAs/AlAs/GaAs with M monolayers of AlAs inside. Following Fu *et al.*[12] we consider the three-band model taking into account mixing of Γ_1 states with the two close-lying bands X_1 and X_3. The electron wave function is written as

$$\Psi_c(\boldsymbol{r}) = w(\boldsymbol{r})|\Gamma_1\rangle + v(\boldsymbol{r})|X_3\rangle + u(\boldsymbol{r})|X_1\rangle, \tag{2.3}$$

where $|\Gamma_1\rangle, |X_3\rangle, |X_1\rangle$ are the corresponding Bloch functions. The envelope functions w, v, u are calculated in the effective-mass approximation. The effective Hamiltonian for Γ-point electrons is determined by the band offset V_0^Γ and effective masses m_A, m_B with the indices A and B corresponding to the GaAs and AlAs layers, respectively. The Hamiltonian of X point electrons is a 2×2 matrix operating on the two-component vector (v, u)

$$H_X = E^{A,B}_{X_1}(z) + \frac{\Delta}{2} + \frac{\hbar^2 k_z^2}{2m_X^\parallel} + \frac{\hbar^2 k_\perp^2}{2m_X^\perp} + \frac{\Delta}{2}\hat{\sigma}_z + Rk_z\hat{\sigma}_y, \tag{2.4}$$

where $E^A_{X_1}$ and $E^B_{X_1}$ are the energies at the X_1 point in the A and B bulk semiconductors, $k_z = -i\partial/\partial z$, the pseudospin matrices $\hat{\sigma}_y$ and $\hat{\sigma}_z$ correspond to the basis $|X_3\rangle, |X_1\rangle$. As in Ref. 12 we neglect for simplicity the difference of $m_X^\parallel$, $m_X^\perp$, Δ, and R in GaAs and AlAs layers, hereafter labeled as A and B, respectively. The Γ-X mixing is included by boundary conditions

$$\begin{aligned} \nabla^A_\Gamma w_A &= \nabla^B_\Gamma w_B + t(z_{if})v_B, \\ \nabla_X v_A &= \nabla_X v_B + t^*(z_{if})w_B. \end{aligned} \tag{2.5}$$

Here z_{if} is the interface coordinate,

$$\nabla^i_\Gamma = a_0\frac{m_0}{m_i}\frac{\partial}{\partial z},\ \nabla_X = a_0\frac{m_0}{m_X^\parallel}\frac{\partial}{\partial z},$$

a_0 is the lattice constant, m_0 is the free electron mass, $i = A, B$. The dimensionless mixing parameter can be written in the form of[12,14]

$$t(z_{if}) = t_{\Gamma X}\exp(2\pi i z_{if}/a_0), \tag{2.6}$$

where $t_{\Gamma X}$ is a real coefficient independent of the interface position. In addition, the envelopes w, v, u and the derivative $\partial u/\partial z$ are assumed to be continuous across heteroboundaries. The general analysis of intervalley mixing in the framework of the effective-mass method is presented in the Appendix.

It should be mentioned that at present there remains some doubt even in the relative ordering of the X_1 and X_3 bands in the bulk AlAs material (see, e.g., Refs. 9 and 15). However, the proposed generalized effective-mass method can be readily applied for band structures with $\Delta_A \neq \Delta_B$. In the following while discussing the results obtained for $\Delta_A = \Delta_B$ we will briefly mention how they are modified if Δ_A and Δ_B differ in sign.

A. k · p interaction between X_1 and X_3 bands neglected

First, we analyze the case $R = 0$ where only Γ_1 and X_3 are mixed. An analytical expression for the transmission coefficient T in this simplified case was obtained by Fu *et al.*[12] using the transfer matrix approach.

Inside the AlAs layer, the X_3 electron envelope function $v(z)$ is a linear combination of $\exp(\pm iqz)$ with $q = [2m_X^\parallel(E - E^B_{X_3})/\hbar^2]^{1/2}$, where E is the kinetic energy of an incoming electron. Outside the AlAs layer, $v(z)$ decays as $\exp(-\sigma|z|)$ with $\sigma = [2m_X^\parallel(E^A_{X_3} - E)/\hbar^2]^{1/2}$. Here E is the electron energy referred to the conduction band bottom in GaAs, $E^{A,B}_{X_3}$ is the position of X_3 minimum in bulk GaAs or AlAs, and we consider the region $E < E^A_{X_3}$. Sewing the solutions inside and outside the AlAs layer at the interfaces together we obtain the r_+, r_- coefficients in Eq. (2.1)

$$r_\pm = -1 + \frac{2ka_0\Sigma_{\mp p}}{(k + iC_\pm\kappa)a_0\Sigma_{\mp p} - it^2_{\Gamma X}(m_X^\parallel m_\Gamma^A/m_0^2)}, \tag{2.7}$$

where $k = (2m_AE/\hbar^2)^{1/2}$, $\kappa = [2m_B(V_0^\Gamma - E)/\hbar^2]^{1/2}$, $p = \mathrm{sgn}(t/t')$, t and t' are the values of $t(z_{if})$ on the left and right interfaces,

$$\begin{aligned} \Sigma_+ &= a_0(\sigma - q\tan\phi_b),\ \Sigma_- = a_0(\sigma + q\cot\phi_b), \\ C_+ &= \tfrac{m_A}{m_B}\tanh\tfrac{\kappa b}{2},\ C_- = \tfrac{m_A}{m_B}\coth\tfrac{\kappa b}{2}, \end{aligned} \tag{2.8}$$

$\phi_b = qb/2$, $b = Ma_0/2$ is the AlAs layer thickness. It is worth to note that the equations of $\Sigma_\pm(E) = 0$ give quantum-confinement energies E_ν of X_3 electrons local-

ized inside the AlAs layer if the Γ-X mixing is neglected. Here the sign $\pm$ corresponds to odd and even values of the level number $\nu = 1, 2, \ldots$. According to Eq. (2.6), when the number M of AlAs monolayers is even, one has $t = t'$ and $\Sigma_{\pm p} = \Sigma_{\pm}$. Thus, for even M the poles of r_+ and r_- are close to the energies E_{2l-1} and E_{2l}, respectively. For energies in the vicinity of E_ν we can expand Σ_+ if ν is odd or Σ_- if ν is even in powers of $E - E_\nu$ as

$$\Sigma_{\pm}(E) \approx 2a_0\sigma_\nu P_\nu (E - E_\nu),$$
$$P_\nu = -\left(1 + \frac{\sigma_\nu^2}{q_\nu^2}\right) \frac{1 + \frac{1}{2}\sigma_\nu b}{4(E_{X_3}^A - E)} . \quad (2.9)$$

It follows from Eqs. (2.7) and (2.9) that allowance for the Γ-X mixing leads to the following complex energies of quasistationary X_3-electron states

$$\tilde{E}_\nu \equiv \tilde{E}_\nu' - i\tilde{E}_\nu'' = E_\nu - t_{\Gamma X}^2 \frac{m_X^{\parallel} m_\Gamma^A}{2m_0^2} \frac{C_\pm \kappa_\nu + ik_\nu}{(C_\pm^2\kappa_\nu^2 + k_\nu^2)\sigma_\nu a_0^2 P_\nu} , \quad (2.10)$$

where $\tau_\nu = \hbar/2\tilde{E}_\nu''$ is nothing more than the escape lifetime of the confined X electron and $\tilde{E}_\nu' - \tilde{E}_\nu$ is the energy renormalization due to the Γ-X mixing.

For odd M, the factors t and t' differ in sign and $\Sigma_{\pm p} = \Sigma_{\mp}$ which means that $r_\pm$ has a pole near E_ν with even or odd ν, respectively.

The above interchange of parities ν can be understood by taking into account that the additional terms in the right-hand side of Eq. (2.5) are equivalent to include the operator (see details in Ref. 12)

$$V_{\Gamma_1 X_3} = a_0 U \sum_{z_l = \pm b/2} \zeta(z_l) \exp\left(2\pi i \frac{z_l}{a_0}\right) \delta(z - z_l), \quad (2.11)$$

into the three-band electron effective Hamiltonian. Here $U = \hbar^2 t_{\Gamma X}/2a_0^2 m_0$, z_l is the heteroboundary coordinate, $\zeta(z_l) = 1$ for the boundary AlAs/GaAs and $\zeta(z_l) = -1$ for the boundary GaAs/AlAs. One can easily verify that for even and odd M the operator (2.11) is, respectively, antisymmetrical and symmetrical under the mirror reflection in the plane σ_z with an origin at the center of the AlAs layer. Therefore, depending on the parity of M, a pair of heteroboundaries at $z_l = \pm b/2$ mixes the envelope functions $w(z)$ and $v(z)$ of opposite parities in case of even M and of identical parities in case of odd M. The symmetry considerations in terms of the whole electron wave function (2.3) can be found in Ref. 14.

It follows from Eq. (2.10) that the escape rate $\Gamma_\nu \equiv \tilde{E}_\nu''/\hbar$ from state $\nu = 1$ is proportional to

$$\Gamma_1 \sim 1 + \frac{t'}{t} \frac{4e^{-\kappa b}}{1 + (m_A k/m_B \kappa)^2} , \quad (2.12)$$

where we retain the term of the first order in $e^{-\kappa b}$ while higher order terms are neglected. Recall that $t'/t = \exp(i\pi M)$ [see Eq. (2.6)]. The dependence of Γ_ν upon the parity of M is explained as follows: The damping of a bound X_3-electron state arises due to the Γ-X mixing at interfaces $\pm b/2$ described by Eq. (2.11). This means that the decay is accompanied by the emission of Γ-electron waves into the GaAs layers. The amplitudes of the Γ-electron waves emitted, say, to the left and induced by the interfaces $-b/2$ and $b/2$ are proportional, respectively, to

$$A \sim t v_\nu(-b/2), \; A' \sim \frac{2e^{-\kappa b}}{1 - ik_\nu m_B/\kappa_\nu m_A} t' v_\nu(b/2), \quad (2.13)$$

where $v_\nu(z)$ is the envelope function. While calculating A' we took into account the exponential decay of the Γ wave in the AlAs layer as well as its reflection on the interface $-b/2$. The second term in the right-hand side of Eq. (2.12) is obtained as a result of the interference between contributions of (2.13) since

$$\Gamma_\nu \sim |A + A'|^2 \approx |A|^2 + 2\mathrm{Re}(A^* A'). \quad (2.14)$$

B. k · p interaction between X_1 and X_3 bands included

Now we consider the general case $R \neq 0$, where R is introduced in the Hamiltonian (2.4). This parameter describes the **k·p** interaction between X_1 and X_3 bands that leads to the camel-back structure of the X_1 conduction band in the bulk GaAs. In this practically important case the coefficients $r_\pm$ are also given by Eq. (2.7), however the expressions for the functions $\Sigma_\pm(E)$ are more complicated. They can be represented in the form

$$\Sigma_\pm = \frac{\sigma_2 - \sigma_1}{Z_\pm} D_\pm, \quad (2.15)$$

$$D_- = a_0^2 \mathrm{Det} \begin{pmatrix} c_1 & c_2 & -1 & -1 \\ \theta_1 s_1 & \theta_2 s_2 & -\tau_1 & -\tau_2 \\ q_1 s_1 & q_2 s_2 & -\sigma_1 & -\sigma_2 \\ \theta_1 q_1 c_1 & \theta_2 q_2 c_2 & \sigma_1\tau_1 & \sigma_2\tau_2 \end{pmatrix}, \quad (2.16)$$

$$Z_- = (\theta_1 q_2 - \theta_2 q_1)(\tau_2 - \tau_1) s_1 s_2 + (\theta_1 s_1 c_2 - \theta_2 s_2 c_1)(\sigma_2\tau_1 - \sigma_1\tau 2),$$

D_+ and Z_+ are obtained by interchange $c_1, c_2 \to s_1, s_2$ and $s_1, s_2 \to -c_1, -c_2$. Here q_1^2 and q_2^2 are roots of the dispersion equation

$$\left(E - E_{X_1}^B - \frac{\Delta}{2} - \frac{\hbar^2 q^2}{2m_X^{\parallel}}\right)^2 = \left(\frac{\Delta}{2}\right) + R^2 q^2 \quad (2.17)$$

for X electrons in bulk AlAs, while $i\sigma_1$ and $i\sigma_2$ satisfy the similar equation for bulk GaAs

$$\left(E - E_{X_1}^A - \frac{\Delta}{2} + \frac{\hbar^2 \sigma^2}{2m_X^{\parallel}}\right)^2 = \left(\frac{\Delta}{2}\right) - R^2\sigma^2. \quad (2.18)$$

For simplicity, we consider here the electron energy region $E_{X_1}^B < E < E_{X_1}^B + \Delta, E_{X_1}^A$, where one of the so-

lutions, q_1^2 and q_2^2, is positive and the other is negative, say q_1 is purely real and q_2 is imaginary. All solutions σ_l of Eq. (2.18) contain both real and imaginary parts. The solutions σ_1 and σ_2 in Eq. (2.16) contain positive real parts and are complex conjugate: $\sigma_2 = \sigma_1^*$. Other notations used in Eq. (2.16) are

$$\theta = \frac{Rq}{E - E_{X_1}^B - \Delta - \hbar^2 q^2/2m_X^{\parallel}},$$
$$\tau = \frac{R\sigma}{E - E_{X_1}^A - \Delta + \hbar^2 \sigma^2/2m_X^{\parallel}}, \qquad (2.19)$$
$$c_l = \cos(q_l b/2),\ s_l = \sin(q_l b/2).$$

Equations $\Sigma_\pm(E) = 0$ [or equivalently, $D_\pm(E) = 0$] determine the quantum-confined states of X electrons in the absence of Γ-X mixing: $\Sigma_+ = 0$ corresponds to the states with an even envelope $v(z)$ and odd envelope $u(z)$ whereas $\Sigma_- = 0$ corresponds to states with $v(z)$ odd and $u(z)$ even. Note that if the X_1 band lies below the X_3 band the lowest level $\nu = 1$ is associated with even $u(z)$ and the parity of the whole wave function $u(z)|X_1\rangle + v(z)|X_3\rangle$ coincides with that of the Bloch function $|X_1\rangle$. The AlAs layer is supposed to be comparatively thin so that the lowest X level $E_{\nu=1}$ lies above $E_{X_1}^B$. For thick enough AlAs layers the level E_1 would lie between the minimum

$$E_{\min} = E_{X_1}^B - \Delta_0 \left[1 + \left(\frac{\Delta}{\Delta_0}\right)^2\right],$$

where $\Delta_0 = R^2 m_X^{\parallel}/2\hbar^2$, and the maximum $E_{X_1}^B$ of the camel-back band structure in bulk AlAs.

C. Energy dispersion of the phases $\phi_\pm$

Figure 2 shows the transmission coefficients for single-barrier heterostructures with the monolayer number M ranging from 8 to 12. The curves are calculated in the effective-mass approximation[12,13] using an improved version of the computer program for $t_{\Gamma X} = 0.5$. The band parameters are the same as in the Ref. 12. In Fig. 2, the incident electron energies lie below the conduction X edge in GaAs so that the transmission probability is contributed by Γ-Γ-Γ, Γ-X-Γ but not by Γ-X-X processes. In order to understand the fine structure in the transmission spectra, we analyze the variation of the phases $\phi_\pm$ with increasing the energy of an incoming electron. They are smooth functions of E except in the narrow regions of the width $\sim \tilde{E}_\nu''$ near the self energies E_ν where either ϕ_+ or ϕ_- rapidly increases by the value up to 2π. The other phase can be considered to be constant within the region so that there exists an energy value satisfying the resonance condition $\phi_+ = \phi_- + \pi(2n+1)$ in which case, according to Eqs. (2.1) and (2.2), the transmission $|T|^2 = 1$ (n is an integer).

Far from the resonant states $e\nu X$ we can neglect the Γ-X mixing and approximate $\phi_\pm$ by

$$\phi_+^\Gamma = 2\arg\left(\cosh\frac{\kappa b}{2} - i\frac{\kappa m_A}{k m_B}\sinh\frac{\kappa b}{2}\right),$$
$$\phi_-^\Gamma = 2\arg\left(\sinh\frac{\kappa b}{2} - i\frac{\kappa m_A}{k m_B}\cosh\frac{\kappa b}{2}\right), \qquad (2.20)$$

taking into account the electron tunneling only via the Γ states of AlAs. Since $\cosh x > \sinh x$, the following inequalities can be written down:

$$-\pi < \phi_-^\Gamma < \phi_+^\Gamma < 0. \qquad (2.21)$$

When increasing $b \to \infty$, ϕ_+^Γ and ϕ_-^Γ tend to the same limiting value of $-2\arctan(\kappa m_A/k m_B)$.

It is clear from the discussion in Sec. II B that if $t' = -t$, r_- has a pole at $\tilde{E}_1$ and the phase ϕ_- exhibits a 2π increase near the energy E_1. Thus, when increasing E the phase ϕ_- first reaches the value of $\phi_+ \approx \phi_+^\Gamma$ where the transmission vanishes and the resonant condition $\phi_- = \phi_+ + \pi$ is achieved at higher energy $\tilde{E}_1'$, so that the transmission zero is followed by the transmission peak (see the spectra in Fig. 2 for $M = 9, 11$). On the other hand, if $t' = t$, the phase ϕ_+ varies rapidly

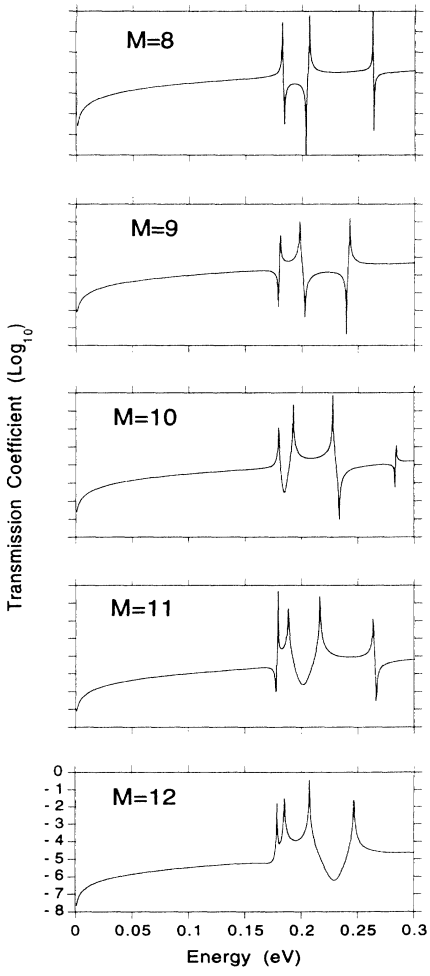

FIG. 2. Electron tunneling transmission coefficients vs incident energy for the GaAs(AlAs)$_M$GaAs heterostructures with M =8–12.

near E_1 and the transmission zero occurs above the energy $\tilde{E}_1'$ (Fig. 2, $M = 8$). It should be mentioned that, for a thick $(AlAs)_M$ layer, the values ϕ_+^Γ and ϕ_-^Γ are so close to each other that the crossing of ϕ_+ and ϕ_- does not occur between E_1 and E_2 and, for M even, the peak is not followed by a zero (Fig. 2, $M = 12$). It can be shown that for a type-I double-barrier structure the transmission spectrum contains resonant peaks but zeros are absent in the transmission because ϕ_+ and ϕ_- have the same asymptotics far from the energies E_ν.

III. TRANSMISSION IN THE PERTURBATION THEORY APPROACH

In this section, we apply the perturbation theory to rederive the formula for the transmission coefficient for energies E close to $\tilde{E}_\nu'$ of a quasibound state ν. Using Fermi's golden rule and the resonant scattering theory one can present the transmission probability for the structures under consideration in the form of

$$|T(k)|^2 = \frac{1}{\hbar v_z}\int_0^\infty dk'\delta(E_{k'} - E_k)\left|\frac{V_{r,\nu}V_{\nu,l}}{E_k - \tilde{E}_\nu' + i\hbar\Gamma_\nu}\right|^2 . \tag{3.1}$$

Here we consider the incidence of an electron with wave vector k from the left to the right, where $E_k = \hbar^2k^2/2m_A, v_z = \hbar k/m_A$, and $\Gamma_\nu = \hbar/\tilde{E}_\nu''$ is the escape rate from the quasibound state ν:

$$\Gamma_\nu = \frac{1}{2\hbar}\int_0^\infty dk(|V_{\nu,l}|^2 + |V_{r,\nu}|^2)\delta(E_k - E_\nu). \tag{3.2}$$

The coupling constant between the bound state and free state in the left lead is defined as

$$V_{\nu,l} = \int \psi_\nu(z)\hat{V}\psi_{lk_\nu}(z)dz, \tag{3.3}$$

where $\psi_\nu(z)$ is the normalized envelope function of state ν, $\hat{V}$ is the perturbation operator,

$$\psi_{lk_\nu}(z) = \begin{cases} e^{ik_\nu(z+z_0)} + r_\nu e^{-ik_\nu(z+z_0)} & \text{for } z < -z_0 \\ (1+r_\nu)e^{-i\kappa_\nu(z+z_0)} & \text{for } z > -z_0, \end{cases} \tag{3.4}$$

$$r_\nu = (1 - if_\nu)/(1 + if_\nu),$$

k_ν, κ_ν, and $f_\nu = (m_A/m_B)(\kappa_\nu/k_\nu)$ correspond to $E = E_\nu$. In a symmetric heterostructure the absolute values of $V_{\nu,l}$ and $V_{r,\nu}$ coincide. For the single-AlAs-layer structure, $z_0 = b/2$, $\psi_\nu(z)$ is a component of the envelope function $v_\nu(z)$ while the perturbation $\hat{V}$ is given by Eq. (2.11), so that in the limit of $\exp(-\kappa_\nu b) \ll 1$ we obtain

$$\begin{aligned} V_{\nu,l} &= -a_0U(1 + r_\nu)v_\nu(-b/2), \\ V_{r,\nu} &= a_0U(1 + r_\nu^*)e^{i\pi M}v_\nu(b/2), \end{aligned} \tag{3.5}$$

where we chose the phase of $t(-b/2)$ in Eq. (2.6) to be zero.

Equation (3.2) for the escape rate can be easily transformed to

$$\Gamma_\nu = \frac{|V_{\nu,l}|^2}{\hbar^2 v_z} . \tag{3.6}$$

Comparing Eq. (3.6) with Eq. (2.10) one obtains for the AlAs-layer structure in the simplified model with $R = 0$

$$|V_{\nu,l}|^2 = \frac{\hbar^2 m_X^\parallel t_{\Gamma X}^2}{2a_0^2 m_0^2 P_\nu}\frac{k_\nu^2}{\sigma_\nu(C_\pm^2\kappa_\nu^2 + k_\nu^2)} . \tag{3.7}$$

Note that Eqs. (3.5) and (3.6) enable one to establish a relation between the envelope function, $v_\nu(z)$, at the heteroboundary and the lifetime, $\tau_\nu = (2\Gamma_\nu)^{-1}$, of the quasistationary state, state ν.

Integrating in Eq. (3.1) over k', using Eq. (3.6) and taking into account that $|V_{r,\nu}|^2 = |V_{\nu,l}|^2$ we arrive to the well-known general expression for the resonant tunneling probability through a symmetric structure

$$|T(k)|^2 = \frac{(\hbar\Gamma_\nu)^2}{(E_k - \tilde{E}_\nu')^2 + (\hbar\Gamma_\nu)^2} . \tag{3.8}$$

In addition to the transmission channel via resonant X states, one can include a contribution to $T(k)$ due to nonresonant tunneling via Γ states of the AlAs layer. If the Γ-Γ-Γ tunneling probability is small, i.e., $\exp(-\kappa_\nu b) \ll 1$, this contribution can be easily taken into account by representing the transmission matrix element in Eq. (3.1) as a sum

$$V_k^\Gamma + \frac{V_{r,\nu}V_{\nu,l}}{E_k - \tilde{E}_\nu' + i\hbar\Gamma_\nu}, \tag{3.9}$$

where

$$V_k^\Gamma = -\frac{4\hbar^2 e^{-\kappa b}k^2\kappa}{m_B(k^2 + m_A^2\kappa^2/m_B^2)} , \tag{3.10}$$

and the total transmission probability can be rewritten in the form of

$$|T(k)|^2 = \left|\frac{4f_\nu}{1+f_\nu^2}e^{-\kappa_\nu b} \pm \frac{\hbar\Gamma_\nu(-1)^M}{E_k - \tilde{E}_\nu' + i\hbar\Gamma_\nu}\right|^2 , \tag{3.11}$$

the sign + or − corresponds to even or odd $v_\nu(z)$. Thus, the energy position, $E_1^{(d)}$, of the E_1-related dip is given by

$$E_1^{(d)} = E_1 + (-1)^M\frac{1+f_1^2}{4f_1}e^{\kappa_1 b}\hbar\Gamma_1 , \tag{3.12}$$

the peak-dip distance being much larger than $\hbar\Gamma_1$ or $|E_1 - \tilde{E}_1'|$.

The relative positions of E_1 and $E_1^{(d)}$ alternate with the increasing M in accordance with the peak-dip sequence in the spectra of Fig. 2.

Figure 3 presents the comparison of our results (solid curves) with ones of Ting and McGill[5] obtained by an empirical eight-band second-neighbor sp^3 tight-binding model (dotted curves). By Fig. 3 we like to emphasize

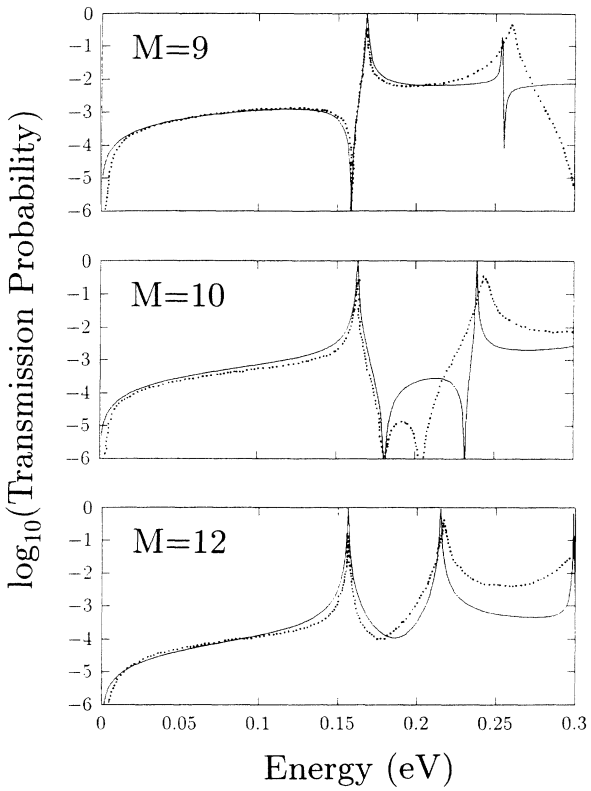

FIG. 3. Electron transmission through the single-barrier structures with M =9,10,12. Dotted curves show the numerical results of Ting and McGill (Ref. 5). Results obtained in the generalized effective-mass method for the optimized set of band parameters are presented by solid curves.

the importance about the phase of mixing term, a vital factor implicitly included in the sophisticated tight-binding method of Ting and McGill.[5] The difference in the peak positions obtained in Refs. 5 and 12 was removed by fitting the band offsets and X-electron longitudinal effective mass $m_X^{\parallel}$: when calculating solid curves in Fig. 3 we took $t_{\Gamma X}=2$, $V_0^{\Gamma}=0.75$ eV, $E_X^0(\mathrm{GaAs})=E_{X_1}^A+\Delta/2=0.5$ eV, $E_X^0(\mathrm{AlAs})=E_{X_1}^B+\Delta/2=0.3$ eV, $m_X^{\parallel}=0.65m_0$ instead of $t_{\Gamma X}=0.5$, $V_0^{\Gamma}=1.1094$ eV, $E_X^0(\mathrm{GaAs})=E_{X_1}^A+\Delta/2=0.5645$ eV, $E_X^0(\mathrm{AlAs})=E_{X_1}^B+\Delta/2=0.3424$ eV, $m_X^{\parallel}=1.68m_0$ used in the calculation of curves in Fig. 2. Thus, a good agreement can be achieved between the transmission spectra calculated by the different methods. However, the final choice of parameters should be made after comparison of theory with relevant experimental data. In the transmission spectra numerically calculated by Ko and Inkson[7] for AlAs single barriers with $M=10$ and 20, the resonance-antiresonance structure is reversed in comparison with Fig. 2 and Eq. (3.12). The opposite peak-dip ordering was also obtained by Schulz[3] for a simplified tight-binding model (an atomic chain with two s-like orbitals per site and nearest-neighbor interaction only). The results of Refs. 3 and 7 can be understood in terms of the generalized effective-mass approximation provided that the X_3 band in bulk AlAs lies lower than the X_1 band, i.e., $\Delta_B<0$. In the tunneling experiments the sharp structures are smeared out due to the contribution to the current from electronic states with different energies (see Sec. IV). However, the analysis of these structures can be used for making comparison between various computation methods.[2–11]

The perturbation theory approach can be readily extended to consider oblique incidence or tunneling through asymmetrical structures. For the oblique incidence, the above results can be used as well if k_ν, κ_ν, E_ν are replaced by

$$\begin{aligned} k_\nu(k_\perp)&=(2m_A E_{\nu k_\perp}/\hbar^2-k_\perp^2)^{1/2},\\ \kappa_\nu(k_\perp)&=[2m_B(V_0-E_{\nu k_\perp})/\hbar^2+k_\perp^2]^{1/2},\\ E_{\nu k_\perp}&=E_\nu+(\hbar^2k_\perp^2/2m_\perp), \end{aligned} \tag{3.13}$$

where $m_\perp$ is the effective mass describing the movement of a confined electron in the (x,y) plane and $k_\perp$ is the in-plane component of the incident electron wave vector, $k_\perp^2=k_x^2+k_y^2$.

IV. TUNNELING CURRENT THROUGH A GaAs(AlAs)$_M$GaAs STRUCTURE

In the following we express the kinetic energy E of an incident electron as the sum $E_{\parallel}+E_\perp$, where $E_{\parallel}=\hbar^2k_z^2/2m_A$ and $E_\perp=\hbar^2k_\perp^2/2m_A$ are associated to the electron motion perpendicular and parallel to interfaces. Knowing the transmission coefficient $T(E_{\parallel},E_\perp)$ one can readily obtain the tunneling current density as

$$j_z=\frac{1}{2\pi^2}\frac{em_A}{\hbar^3}\int dE_{\parallel}dE_\perp|T(E_{\parallel},E_\perp)|^2(F^l-F^r), \tag{4.1}$$

where $F^{l,r}$ are the electron distribution functions in the left and right leads, which is described at low temperatures by the step functions

$$F^l=\Theta(E_F-E),\ F^r=\Theta(E_F+eV-E),$$

E_F being the Fermi energy and V being the bias between the leads. We take $V>0$ so that the product eV is negative. We consider the region of electric fields where the level E_{e1X} is tuned to resonance with the left-lead states occupied by the degenerate electron gas and F^r in Eq. (4.1) can be put zero. The current is calculated self-consistently taking into account the electrostatic field induced by the electrons temporarily confined inside the AlAs layer. The whole electrostatic potential $\phi(z)$ is determined from the Poisson equation

$$\frac{d^2\phi}{dz^2}=-\frac{4\pi N_1}{\epsilon}[u_1^2(z)+v_1^2(z)], \tag{4.2}$$

where N_1 is the two-dimensional density of the confined electrons. The structure is assumed to contain GaAs spacers of effective thicknesses L_l and L_r on both sides of the (AlAs)$_M$ layer. The boundary conditions for the potential $\phi(z)$ are taken as

$$\phi(-L_l-b/2)=0,\ \phi(L_r+b/2)=V, \tag{4.3}$$

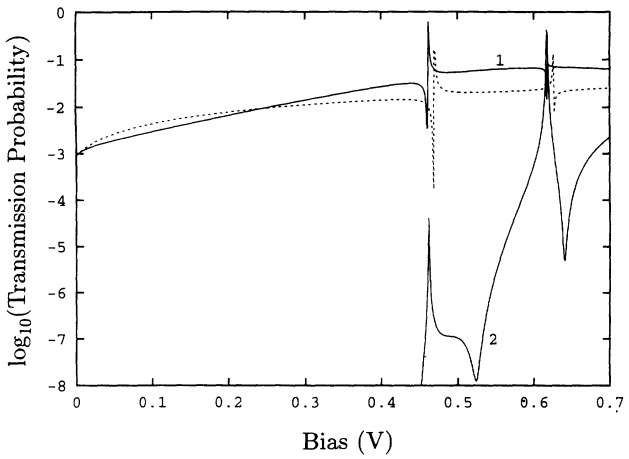

FIG. 4. Transmission coefficients vs applied bias through a five monolayer AlAs barrier for an electron normally incident from the GaAs lead with the initial energy 10 meV (solid curves). The effective spacer thicknesses are taken to be $L_l = 30$ Å and $L_r = 50$ Å. The curves 1 and 2 present, respectively, probabilities of transfer between the GaAs Γ_1 state on the left into the GaAs Γ_1 and X states on the right. The dashed curve is the transmissivity through the unbiased structure as a function of the equivalent potential $V = [(E - 10\text{ meV})/|e|](L_l + b + L_r)/(L_l + b/2)$, where E is the incident electron energy.

the origin $z = 0$ being chosen at the center of the AlAs layer.

Figure 4 shows the bias dependence of transmission probabilities via the structure with $M = 5$, $L_l = 30$ Å, $L_r = 50$ Å for the initial kinetic electron energy $E = 10$ meV. In accordance with the definition of the spacer effective thicknesses, the electric field is assumed to be uniform along the whole structure $L_l + b + L_r$. While calculating the transmission we took into account both Γ-Γ-Γ, Γ-X-Γ and Γ-Γ-X, Γ-X-X channels. In Fig. 4 the solid curves 1 and 2 represent separate contributions due to transmissions into Γ and X states. The set of structure parameters was the same as for Fig. 2. One can see that the resonance and antiresonance pairs are present in the transmissivity-bias curves and the relative position of peaks and dips is parity dependent. The opposite peak-dip sequence obtained in similar curves by Boykin and Harris[4] can be related to the above-mentioned problem of the ordering of the X_1 and X_3 states.

It follows from Fig. 4 that for the chosen set of band parameters the contributions from Γ-X-X and Γ-Γ-X channels are comparatively small in the region of the first resonance and hereafter we neglect these contributions. For comparison we also present in Fig. 4 the transmission spectrum (dashed curve) of the unbiased structure plotted versus the equivalent bias

$$V = \frac{1}{|e|}(E - 10)\frac{L_l + b + L_r}{L_l + b/2},$$

where E is the electron initial energy in meV. One can see that the dashed curve is close to curve 1, the small difference in peak positions being just connected with the Stark shift of the quasibound X levels. This allows one to neglect in the following calculation the reflection of electron waves from the spacer areas.

Note that in the narrow resonant regions of $|E - E_\nu| < \hbar\Gamma_\nu$, the nonresonant contribution in Eq. (3.11) is negligible while in off-resonant regions V_k^Γ can dominate if the AlAs layer is not very thick. Thus, the resonant and nonresonant contributions to the tunneling current can be calculated separately. When calculating the nonresonant background current one should obtain the usual exponential-like dependence on the applied bias. In the following for simplicity we take into consideration only the resonant contribution to $|T(E_\parallel, E_\perp)|^2$.

The spectral dependence of $|T(E_\parallel, E_\perp)|^2$ can be approximately expressed in the form of

$$|T(E_\parallel, E_\perp)|^2 = \frac{(\hbar\Gamma_1)^2}{[E_\parallel + E_\perp(1 - m_A/m_X^\perp) - E_1 - e\phi_0]^2 + (\hbar\Gamma_1)^2}, \tag{4.4}$$

where

$$\phi_0 = \int dz\, \phi(z)[u_1^2(z) + v_1^2(z)],$$

$m_X^\perp$ is the in-plane effective mass of an X electron. For normal incidence $|T(E_\parallel, 0)|^2$ reduces to the resonant contribution to the transmission probability given by Eq. (3.11). Substituting Eq. (4.4) into Eq. (4.1) and taking into account that for small enough escape rate of Γ_1, the transmission spectrum (4.4) can be rewritten as

$$\pi\hbar\Gamma_1\delta[E_\parallel + E_\perp(1 - m_A/m_X^\perp) - E_1 - e\phi_0], \tag{4.5}$$

we obtain

$$j_z = \frac{1}{2\pi}\frac{em_A}{\hbar^2}\int_0^{\bar{E}_\perp} dE_\perp \Gamma_1(E_\perp), \tag{4.6}$$

where the upper limit is

$$\bar{E}_\perp = \begin{cases} 0 & \text{if } E_1 + e\phi_0 < 0 \text{ or } E_1 + e\phi_0 > E_F \\ (E_1 + e\phi_0)/(1 - m_A/m_X^\perp) & \text{if } 0 < E_1 + e\phi_0 < (1 - m_A/m_X^\perp)E_F \\ (m_X^\perp/m_A)[E_F - (E_1 + e\phi_0)] & \text{if } (1 - m_A/m_X^\perp)E_F < E_1 + e\phi_0 < E_F. \end{cases} \tag{4.7}$$

Neglecting the variation of $\Gamma_1(E_\perp)$ within the energy interval of the width E_F we have

$$j_z = \frac{1}{2\pi}\frac{em_A}{\hbar^2}\bar{E}_\perp(\phi_0)\Gamma_1. \tag{4.8}$$

In the same approximation j_z and N_1 are connected by a simple relation

$$j = eN_1\Gamma_1/2. \tag{4.9}$$

Taking into account Eq. (4.9) we obtain a final I-V characteristic

$$j(V) = j_0 \begin{cases} 0 & \text{if } V < V_{\min} \text{ or } V > V_{\max} \\ (V - V_{\min})/(V' - V_{\min}) & \text{if } V_{\min} < V < V' \\ (V_{\max} - V)/(V_{\max} - V') & \text{if } V' < V < V_{\max}. \end{cases} \tag{4.10}$$

Here

$$j_0 = \frac{1}{2\pi}\frac{em_A}{\hbar^2}\Gamma_1 E_F,\ V_{\min} = \frac{E_1 - E_F}{|e|\xi}\ ,\ V_{\max} = \frac{E_1}{|e|\xi}\ ,$$

$$|e|\xi V' = E_1 - E_F\left\{1 - \frac{m_A}{m_X^{\perp}} - \frac{e^2 m_A}{\pi\hbar^2} \times \left[\frac{2\pi}{\epsilon}\xi(L_r - L_l) + \bar{\phi}_0\right]\right\},$$

$$\xi = (L_l + b/2)(L_l + L_r + b).$$

For convenience we introduced the function $\bar{\phi}(z)$ so that $eN_1\bar{\phi}(z)$ is an even solution of Eq. (4.2) with the boundary condition $\bar{\phi}(-L_l - b/2) = 0$. Due to screening in the heavily doped leads $\phi(z) = 0$ for $z < -L_l - b/2$, and $\phi(z) = V$ for $z > L_r + b/2$,

$$\phi(z) = eN_1\bar{\phi}(z) + [V - eN_1\bar{\phi}(L_r + b/2)]\frac{z + L_l + b/2}{L_l + L_r + b} \tag{4.11}$$

inside the interval between $-L_l - b/2$ and $L_r + b/2$. One can see that $\bar{\phi}(z)$ is independent on the applied bias,

$$\bar{\phi}_0 = \int dz\, \bar{\phi}(z)[u_1^2(z) + v_1^2(z)].$$

Figure 5 shows the shape of the resonant $j(V)$ curve neglecting (dashed line) and including the self-consistent potential influence (solid line). We use the notation $|e|\xi V_0' = E_1 - E_F(1 - m_A/m_X^{\perp})$.

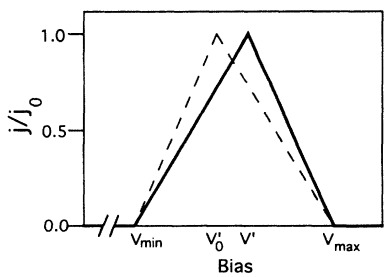

FIG. 5. The shape of the resonant tunneling current through the single-barrier structure vs the applied bias neglecting (dashed) and including the self-consistent potential influence (solid line).

In general the parameters of a heterostructure can be such that V' exceeds $V_{\max}$, in which case the current-voltage dependence exhibits an intrinsic bistability.

V. SUMMARY

We have proposed an approach to calculate the electron reflectivity and transmissivity in a symmetrical multilayer structure. The approach is based on splitting the problem into simpler auxiliary problems for even and odd solutions. The analytical properties of the transmission spectra have been analyzed in the vicinity of the structure quasistationary bound states.

We have calculated tunneling probability as a function of electron energy across a single-barrier structure $GaAs(AlAs)_M GaAs$ within the generalized effective-mass approximation. The intervalley mixing at the interfaces is included in the boundary conditions which depend on the parity of monolayer number M so that the latter becomes an additional parameter of the problem. As a result, the fine structure of transmission spectra is sensitive not only to the value of integer M but also to its parity. It seems that the existing controversy in literatures concerning the calculated peak-dip sequence is connected with the uncertainty of model parameters and accuracy of numerical calculations. Our effective-mass-method calculations show the reversal of ordering between, say, the lowest peak and its satellite dip with the sign inversion of the X_1-X_3 splitting, Δ_B. In this connection, we attach much importance to a reliable determination of the bulk AlAs band structure near the X point.

We have analyzed the parity-dependent effects in a biased AlAs single-barrier structure. As well as in the transmission spectra, the peak-dip sequence in transmission vs bias curves is sensitive to the parity of M and the sign of Δ_B.

An analytical form of current-voltage characteristics has been obtained taking into account the self-consistent electrostatic potential due to the space charge stored inside the AlAs layer. Due to contributions to the current from electron states with different energies, the parity of M has no remarkable influence on the shape of I-V X-resonant peaks.

We expect the parity-dependent effects to be more pronounced for intersubband or interband absorption respectively in n-type and intrinsic GaAs/AlAs superlattices near the type-I–type-II transition[12,17] and to influence electron quasibound-state lifetimes in GaAs/AlAs

double-barrier heterostructures.[5] All these effects can be described in the generalized effective-mass formalism developed in the previous[12] and present papers. The formalism can be further improved to include factors like the nonparabolicity in bands. We can also extend the work to study the Γ-L mixing in $Ga_xAl_{1-x}Sb/GaAs$ system provided that the basic physical parameters are known. Nevertheless the fundamentals remain the same.

APPENDIX

Here we present a general approach to solve the problem of intervalley mixing in heterostructures in the effective-mass method. Evidently, two electron states with the wave vectors $\mathbf{K}_1$ and $\mathbf{K}_2$ can be mixed at a heterointerface with the normal $\mathbf{N}$ if there exists a three-dimensioanl (3D) reciprocal-lattice vector $\mathbf{b}$ which satisfies the equation

$$(\mathbf{K}_1 - \mathbf{K}_2 - \mathbf{b})_\perp = 0. \tag{A1}$$

Here $\perp$ means the in-plane component of a vector. The wave vector conservation law in the $\mathbf{N}$ direction is removed because the translational symmetry is broken in this direction due to the presence of interface.

The $\mathbf{K}_i$-valley-related electron wave function can be compactly written in the generalized effective-mass approximation as

$$\Psi_i(\mathbf{r}) = \sum_l \psi_{il}(\mathbf{r})|\mathbf{K}_i, l\rangle, \tag{A2}$$

where $i = 1, 2$, $|\mathbf{K}_i, l\rangle$ are the Bloch functions at the $\mathbf{K}_i$ point and $\psi_{il}(\mathbf{r})$ are the envelopes. The index l takes into account the possible complex band structure, in particular the band degeneracy or close-lying bands.

The boundary conditions at the A-B interface can be expressed in the form of

$$\begin{pmatrix} \psi_1^{\mathbf{A}} \\ \nabla_1^A \psi_1^{\mathbf{A}} \\ \psi_2^{\mathbf{A}} \\ \nabla_2^A \psi_2^{\mathbf{A}} \end{pmatrix} = \begin{pmatrix} \hat{T}_{11} & \hat{T}_{12} \\ \hat{T}_{21} & \hat{T}_{22} \end{pmatrix} \begin{pmatrix} \psi_1^{\mathbf{B}} \\ \nabla_1^B \psi_1^{\mathbf{B}} \\ \psi_2^{\mathbf{B}} \\ \nabla_2^B \psi_2^{\mathbf{B}} \end{pmatrix}, \tag{A3}$$

where $\psi_i(\mathbf{r})$ is the column with the components $\psi_{i1}(\mathbf{r})$, $\psi_{i2}(\mathbf{r})\ldots$, $\nabla_i^{A,B} = a_0(m_0/m_i^{A,B})(\partial/\partial z)$, z is the coordinate in the $\mathbf{N}$ direction, a_0 is the lattice constant, m_0 is the free electron mass, $m_i^{A,B}$ is the effective mass of electron in the $\mathbf{K}_i$ valley along $\mathbf{N}$. The interface matrix $\hat{T}$ is dimensionless, its submatrix $\hat{T}_{ii'}$ connects the values of $\psi_i^{\mathbf{A}}, \nabla_i^A \psi_i^{\mathbf{A}}$ with $\psi_{i'}^{\mathbf{B}}, \nabla_{i'}^B \psi_{i'}^{\mathbf{B}}$: $\hat{T}_{ii}$ describe boundary conditions for the $\mathbf{K}_i$-valley envelope functions while $\hat{T}_{12}$ and $\hat{T}_{21}$ describe the intervalley mixing effects at the heteroboundaries. In order to include the different translational properties of the Bloch functions $\mathbf{K}_1$ and $\mathbf{K}_2$ one should impose the following relations:

$$\begin{aligned} \hat{T}_{ii}(z_2) &= \hat{T}_{ii}(z_1), \\ \hat{T}_{12}(z_2) &= \exp[i(\mathbf{K}_1 - \mathbf{K}_2 - \mathbf{b})_\parallel (z_2 - z_1)]\,\hat{T}_{12}(z_1), \\ \hat{T}_{21}(z_2) &= \exp[-i(\mathbf{K}_1 - \mathbf{K}_2 - \mathbf{b})_\parallel (z_2 - z_1)]\,\hat{T}_{21}(z_1) \end{aligned} \tag{A4}$$

between the $\hat{T}$ matrices for the two equivalent interfaces z_1 and z_2 with

$$z_2 - z_1 = \sum_{j=1}^{3} n_j a_j^\parallel.$$

Here $\mathbf{a_j}$ are the basic translational vectors of the 3D crystal lattice and n_j are integers, the symbol $\parallel$ means the component of a 3D vector parallel to the structure principal axis $z \parallel \mathbf{N}$. Thus, the description of intervalley mixing in the generalized effective-mass approximation assumes an explicit dependence of boundary conditions on the valley wave vectors.

The possible ambiguity in the choice of the vector $\mathbf{b}$ from Eq. (A1) makes no influence on the relations (A4). Really, if the other reciprocal lattice vector $\mathbf{b}'$ satisfes Eq. (A1) then $(\mathbf{b} - \mathbf{b}')_\perp = 0$ and the product

$$(\mathbf{b} - \mathbf{b}')_\parallel (z_2 - z_1) = (\mathbf{b} - \mathbf{b}') \cdot \left(\sum_{j=1}^{3} n_j \mathbf{a}_j \right)$$

is an integer of 2π.

Note that the above simple considerations can be readily modified to take into account the lattice constant mismatch and intrinsic strain in multilayer heterostructures.

Following the general procedure for the particular case of Γ-X mixing in (001)-oriented A_3B_5 heterostructures we have $\mathbf{K}_\Gamma = 0$, $\mathbf{K}_\mathbf{X} = (0, 0, 2\pi/a_0)$, Eq. (A1) can be satisfied with $\mathbf{b} = 0$, and Eq. (A2) reduces to $\Psi_\Gamma(\mathbf{r}) = w(\mathbf{r})|\Gamma_1\rangle$, $\Psi_X(\mathbf{r}) = v(\mathbf{r})|X_3\rangle + u(\mathbf{r})|X_1\rangle$. For the zinc-blende structure the basic vectors can be chosen in the form of $\mathbf{a}_1 = (a_0/2)(1, 1, 0)$, $\mathbf{a}_2 = (a_0/2)(0, 1, 1)$, and $\mathbf{a}_3 = (a_0/2)(1, 0, 1)$. Therefore, $z_2 - z_3 = (n_2 + n_3)a_0/2$, $(\mathbf{K}_\Gamma - \mathbf{K}_\mathbf{X} - \mathbf{b})_\parallel (z_2 - z_1) = (n_2 + n_3)\pi$, and the mixing coefficients in submatrices $\hat{T}_{\Gamma X}$, $\hat{T}_{X\Gamma}$ change their signs if the interface z_2 is shifted by one monomolecular layer along the principal axis $z \parallel [001]$.

[1] L.J. Sham and Y.-T. Lu, J. Lumin. **44**, 207 (1989).
[2] K.V. Rousseau, K.L. Wang, and J.N. Schulman, Appl. Phys. Lett. **54**, 1341 (1989).
[3] P.A. Schulz, Phys. Rev. B **44**, 8323 (1991).
[4] T.B. Boykin and J.S. Harris, Jr., J. Appl. Phys. **72**, 988 (1992).
[5] D.Z.-Y. Ting and T.C. McGill, Phys. Rev. B **47**, 7281 (1993).
[6] A.C. Marsh, Semicond. Sci. Technol. **1**, 320 (1986).
[7] D.Y.K. Ko and J.C. Inkson, Semicond. Sci. Technol. **3**, 791 (1988); Phys. Rev. B **38**, 9945 (1988).
[8] H.C. Liu, Appl. Phys. Lett. **51**, 1019 (1987).

[9] T. Ando and H. Akera, Phys. Rev. B **40**, 11 619 (1989).
[10] J.-B. Xia, Phys. Rev. B **41**, 3117 (1990).
[11] Y. Carbonneau, J. Beerens, L.A. Cury, H.C. Liu, and M. Buchanan, Appl. Phys. Lett. **62**, 1955 (1993).
[12] Y. Fu, M. Willander, E.L. Ivchenko, and A.A. Kiselev, Phys. Rev. B **47**, 13 498 (1993).
[13] E.L. Ivchenko, A.A. Kiselev, Y. Fu, and M. Willander, Solid-State Electron. **37**, 813 (1994).
[14] I.L. Aleiner and E.L. Ivchenko, Fiz. Tekh. Poluprovodn. **27**, 594 (1993) [Sov. Phys. Semicond. **27**, 330 (1993)].
[15] T. Ando, Phys. Rev. B **47**, 9621 (1993).
[16] A.G. Aronov and E.L. Ivchenko, Fiz. Tverd. Tela Leningrad **34**, 948 (1992) [Sov. Phys. Solid State **34**, 507 (1992)].
[17] V. Voliotis, R. Grousson, P. Lavallard, E.L. Ivchenko, A.A. Kiselev, and R. Planel, Phys. Rev. B **49**, 2576 (1994).